

ANALYSIS OF SOLAR INTEGRATED SYMMETRICAL HYBRID SWITCHED-INDUCTOR DC-DC CONVERTER FED SRM DRIVE FOR ELECTRIC VEHICLE APPLICATION

RAVI KIRAN DASARI,

Research Scholar, Department of EEE, Sathyabama Institute of Science and Technology (Deemed to be University), Chennai, India

D. GODWIN IMMANUEL

Professor, Department of EEE, Sathyabama Institute of Science and Technology (Deemed to be University), Chennai, India

Abstract

In profound applications like photovoltaic systems, smart lighting systems and automobile sector, high gain DC-DC converters are pioneered to step-up the low voltage level to high voltage. Classical Boost converter is limited with its voltage gain owing to the efficiency of the system and current ripples. This paper presents a genre of Symmetrical Hybrid Switched Inductor Boost converter powered from a solar photovoltaic system for high step-up voltage conversion ratio. The topological root of the Symmetrical Hybrid Switched Inductor Boost converter is from the combination of active and passive units. The converter is analyzed, compared with existing topologies and details are presented. The Symmetrical Hybrid Switched Inductor Boost converter output is connected to Switched Reluctance Motor to drive the wheels of an electric vehicle. The coils of 6/4 SRM is fed from Asymmetrical converter. The proposed system is analyzed and results are shown using MATLAB/SIMULINK software.

Index Terms: Symmetrical Hybrid Switched Inductor Boost converter, Electric Vehicle, Photo-Voltaic (PV), DC-DC Converters, Switched reluctance motor (SRM), motor drive.

1. INTRODUCTION

Energy from photovoltaic (PV) system has gained interest in recent years and is capable of solving the energy crisis. Solar PV system is one of the prominent part of renewable resources. Energy from PV system has become most reliable source because of its free and infinite power. Many advantages including zero pollution, production cost, availability and life-span [1-2]. One main concern of PV system is its low output voltage and in many electrical applications, this low voltage is not sufficient to drive the load. To avoid this nature of PV system, either PV modules are to be connected in series or to use DC-DC converters to meet the load requirements.

Traditional step-up converters give high voltage gain by increasing duty cycle but at the loss of efficiency with high current ripples. Many DC-DC converter topologies have been developed to give high voltage gain with slight duty cycle. Isolated DC-DC converters increase the turns ratio to give out high gain [3-7]. Isolated converters, extracted from Buck Converter, and reflect high input current ripple and high voltage stress across output diode. Isolated converters, extracted from Boost Converter, reflects voltage spike across switch which generated from leakage inductance [8-10]. Non-Isolated DC-DC converters yields high voltage ratio with good efficiency. Coupled inductor type Isolated DC-DC can give out high voltage gain by increasing the turns ratio [11-16]. The leakage inductance is unavoidable in Coupled inductor type Isolated type of converters and can cause high spike

in voltage, stressing the switch during turn-off [17-18]. Non-coupled inductor type Isolated type of converters can yield high gain with less magnetic components [19-22].

Different topologies pertaining to switched-inductor and switched-capacitor with extended range of voltage gain are furnished in [23-28]. With the adaption of series and parallel switched-inductor cells, high voltage gain ration can be achieved. This paper presents a genre of Symmetrical Hybrid Switched Inductor Boost (SH-SL) converter [28-29] with the combination of active and passive units. SH-SL converter is powered from a solar PV system. Freely available energy like solar-PV systems [30-33] can drive the traction motor [34] of electric vehicle (EV). EVs run by emitting zero air pollution and can replace the polluting scenario with conventional vehicles. Ferrite materials with high magnetic permeability and low coercive motors have gained importance these days, replacing permanent magnet machines. Switched reluctance motor (SRM), which is capable of running at high speeds [35-36] with simple construction, is suitable to drive EV.

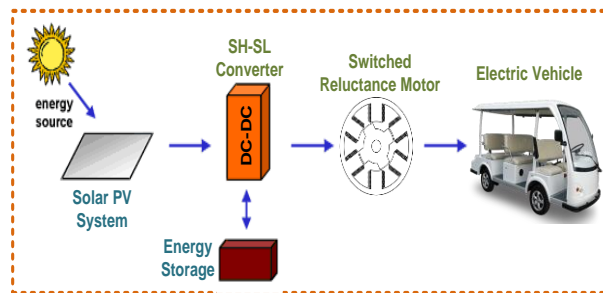


Fig. 1. Block diagram of the system

This paper presents a genre of Symmetrical Hybrid Switched Inductor Boost converter powered from a solar photovoltaic system for high step-up voltage conversion ratio. The topological root of the Symmetrical Hybrid Switched Inductor Boost converter is from the combination of active and passive units. The converter is analyzed, compared with existing topologies and details are presented.

The Symmetrical Hybrid Switched Inductor Boost converter output is connected to Switched Reluctance Motor to drive the wheels of an electric vehicle. The block diagram of the system is shown in figure 1.

I. SYMMETRICAL HYBRID SWITCHED INDUCTOR BOOST CONVERTER

A. Symmetrical Hybrid Switched Inductor Boost Converter Representation

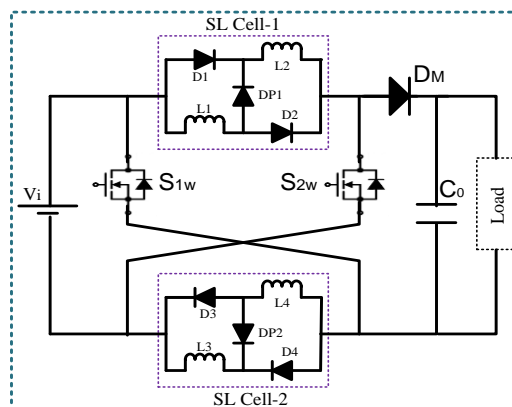


Fig.2. SH-SL Boost converter

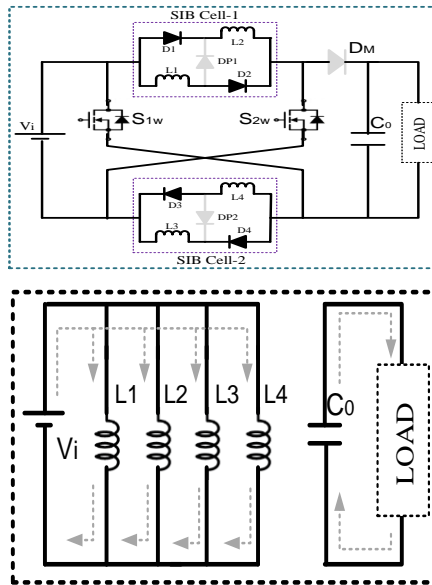


Fig. 3. SH-SL converter in Mode-1

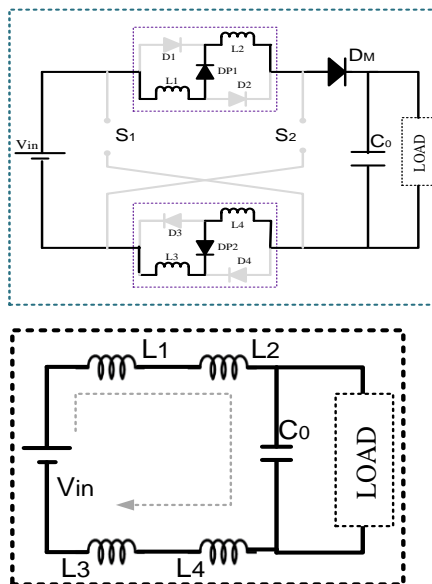


Fig. 4. SH-SL converter in Mode-2

Figure 2 shows the schematic circuit of symmetrical Hybrid Switched Inductor (SH-SL) Boost converter. SH-SL converter is formed by combining active and passive switched-inductor (SL) units. Such units are shown as SL cell-1 and SL cell-2 in Figure 2. Each SL cell consists of two inductors and three diodes. SH-SL converter consists of two power switches S_{1w} and S_{2w} , generally MOSFETs, and output capacitor.

High gain is achieved by clamping active and passive units. The inductors, by turning ON two power switches, form an active SL unit (mode-1 of operation). The SL cell with three diodes and two inductors with two power switches turned OFF forms passive SL unit (mode-2 of operation). The modes of operation of SH-SL converter under continuous conduction mode (CCM) are explained below and the analysis is carried out considering equal inductance values. SH-SL Converter Modes in CCM Operation

Mode-1: Both the switches S1w and S2w are turned ON. The elements form an active SL unit and the input voltage presents across inductors. Inductors L1 to L4 shapes to parallel and are imposed to input voltage level. Capacitor discharges and acts as source to the load. The current flow path and the equivalent circuit are shown in Figure 3. The voltage across inductor is expressed as:

$$V_i = V_{L1} = V_{L2} = V_{L3} = V_{L4} \quad (1)$$

Mode-2: Both switches S1w and S2w are OFF. The elements form a passive SL unit and the four inductors L1, L2, L3 and L4 are discharged to the output forming a series circuit. The current flow path and the equivalent circuit is shown in figure 4. Voltage across the inductor (L1=L2=L3=L4) is given by (2).

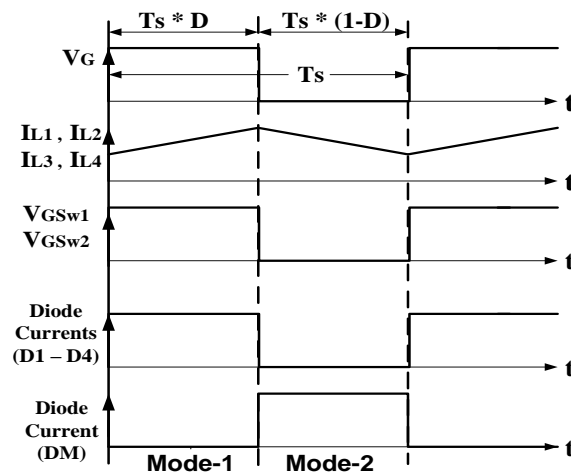


Fig.5. Continuous Mode device characteristics of SH-SL converter

$$V_L = \left(\frac{V_{in} - V_0}{4} \right) \quad (2)$$

The operational timing diagram of is detailed in Figure 5 for SH-SL converter in CCM operation. The gain of hybrid boost converter using equations (1) and (2) is:

$$\frac{V_{in} * DT_s + \left(\frac{V_{in} - V_0}{4} \right) (1-D) T_s}{T_s} = 0 \quad (3)$$

$$V_{gain} = \frac{V_0}{V_{in}} = \frac{1+3D}{1-D} \quad (4)$$

Duty cycle formulation, equation (4) is modified as

$$(1 - D) * V_0 = (1 + 3D) * V_{in} \quad (5)$$

$$D = \frac{V_0 - V_{in}}{V_0 + 3V_{in}} \quad (5)$$

$$\frac{V_{in} * DT_s + \left(\frac{V_{in} - V_0}{2} \right) (1-D) T_s}{T_s} = 0 \quad (6)$$

$$V_{gain} = \frac{V_0}{V_{in}} = \frac{1+D}{1-D} \quad (7)$$

Furthermore, equation (7) is modified as

$$(1 - D) * V_0 = (1 + D) * V_{in} \quad (8)$$

$$D = \frac{V_0 - V_{in}}{V_0 + V_{in}} \quad (8)$$

B. Analysis of SH-SL Converter

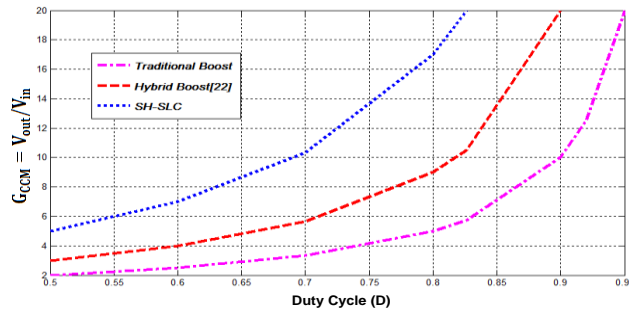


Fig.6. Duty cycle versus voltage gain comparison

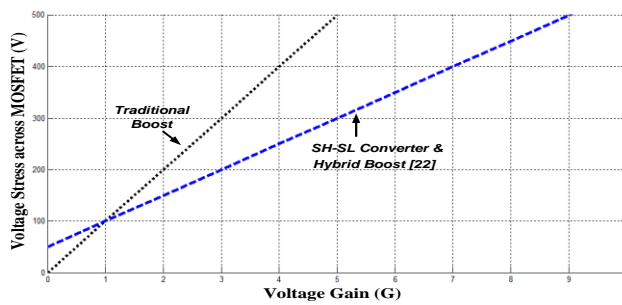


Fig.7. Voltage stress comparison

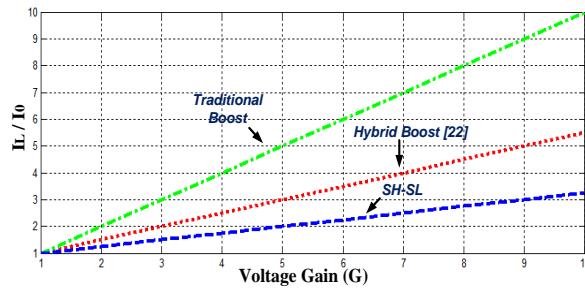


Fig. 7. Inductor current comparison

With different inductor values in SH-SL converter, the voltage stress across switch increases and thus analysis with equal inductance is considered. With equal inductor topology, the inductors can be integrated with single core which lessens the size of magnetic components. The gain in voltage is shown in figure 5. Gain is high and high output voltage is obtained with less duty cycle which eventually reduces the current ripple and current stress on the components. Voltage stress across the main switch is less compared to existing topology as shown in figure 6 and efficiency increases with less cost. Figure 7 shows the average inductor current and the amount of current through inductor is less.

C. Design of SH-SL Converter

SH-SL converter is designed to operate with 100V input and 500V output. The operating frequency of the converter is considered to be 10 KHz and power rated at 1KW.

Duty Cycle of converter for 100V input and 500V output voltage values, the duty cycle (D) is calculated as 50%.

Inductance $L=10$ mH

Capacitance $C=10\mu$ F

Table-1 illustrates parametric design of Hybrid Boost converter. Table-2 shows the comparative illustration of SH-SL converter with existing converters.

TABLE I: HYBRID BOOST CONVERTER PARAMETERS

Parameter	Value
Input source Voltage, V_{in}	100V
Output Voltage, V_o	500V
Power, P	1 KW
Switching Frequency, F_s	10KHz
Inductor Current ripple, ΔI_L	0.5 A
Capacitor Voltage ripple, ΔV_C	10 V
Inductor, L	10 mH
Capacitor, C	10 μ F

TABLE II: COMPARATIVE CHART

Parameter	Traditional Boost	Hybrid Boost [22]	SH-SL
Voltage Gain	$\frac{1}{1-D}$	$\frac{1+D}{1-D}$	$\frac{1+3D}{1-D}$
Number of Diodes	1	1	7
Number of MOSFETs	1	2	2
Voltage across MOSFET	GV_{in}	$\frac{(G+1)V_{in}}{2}$	$\frac{(G+1)V_{in}}{2}$
Voltage across Output Diode	GV_{in}	$(G+1)V_{in}$	$(G+1)V_{in}$
Current through Inductor (I_L)	GI_0	$\frac{(G+1)I_0}{2}$	$\frac{(G+3)I_0}{4}$

II. PV WITH SH-SL CONVERTER FED SRM DRIVE

A. PV System with SH-SL Converter

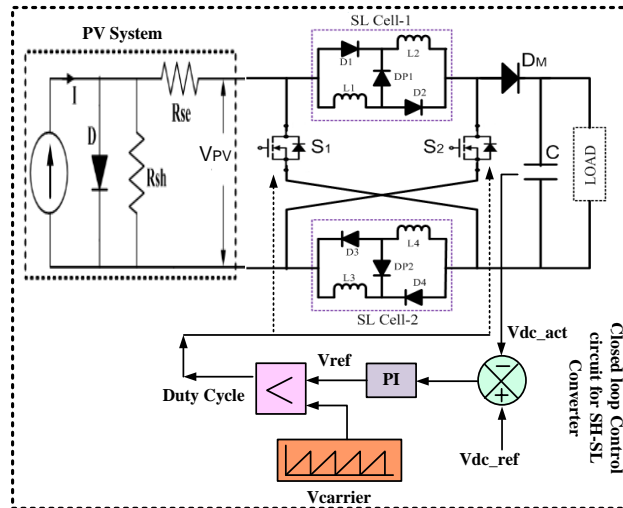


Fig 8. PV with SH-SL converter

PV system doesn't give out voltage level which is suitable to drive any load. PV system insists for DC-DC boost converter to increase its voltage level at user point. Figure 8 illustrates PV system with SH-SL converter. The output of the PV system is connected to SH-SL converter and the load parameters of the SH-SL converter are fed back to controller to generate gate pulses to switches of the converter. With this loop operation, desired output of DC-DC converter can be achieved.

B. SRM with Asymmetrical Converter

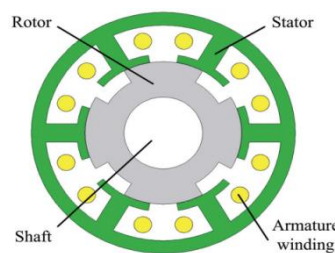


Fig. 9. Three-Phase 6/4 SRM

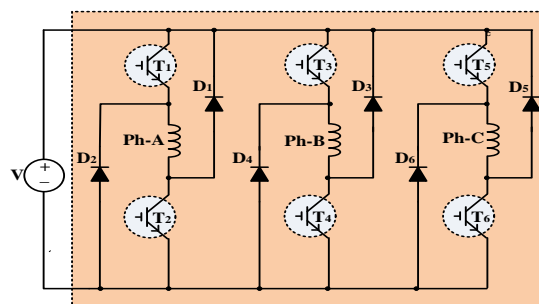
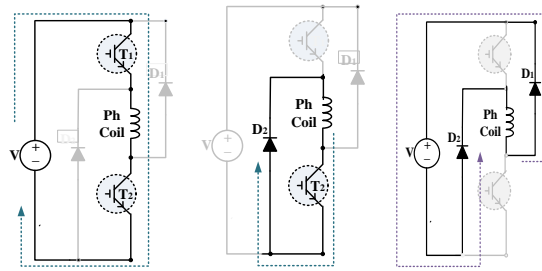


Fig.10. Conventional asymmetrical structure converter for SRM



(a) Excitation (b) Free-wheeling (c) Regeneration

Fig. 11. Operating modes of SRM

Constructional view of SRM is shown in figure 9 and the converter exciting the phases of SRM is shown in figure 10. The three modes – excitation, free-wheeling and regeneration are represented in figure 11. Robust and simple construction makes SRM suitable for many applications. Its high speed capability suits for EV. By sequentially switching (as in figure 11) the power switches in asymmetrical converter, SRM can be operated in three modes.

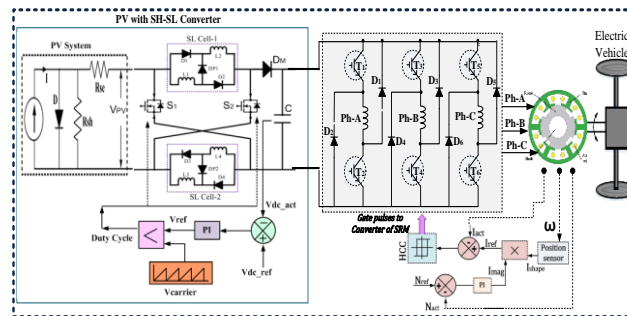


Fig. 12. Solar with Hybrid Boost Converter and SR Motor Drive

C. PV with SH-SL Converter with Switched Reluctance Motor Drive for Electric Vehicle application

Photo-voltaic system with SH-SL converter to feed the SRM for EV application is shown in figure 12. The output of the PV system is given as an input to the SH-SL converter which increases the voltage level. The output of the converter is fed to asymmetrical converter to excite the stator coils of SRM to generate flux to align the rotor. SRM drive is in feedback mode where the respective control operation takes place and speed is adjusted according to the desired value.

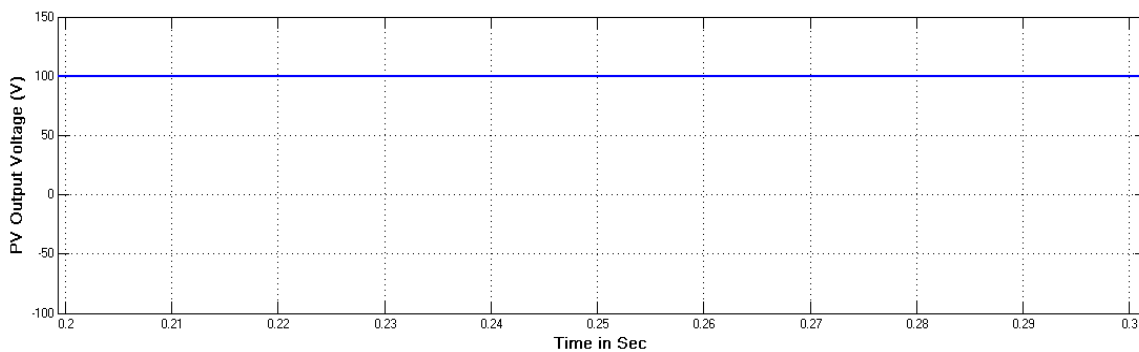


Fig. 13. PV output voltage

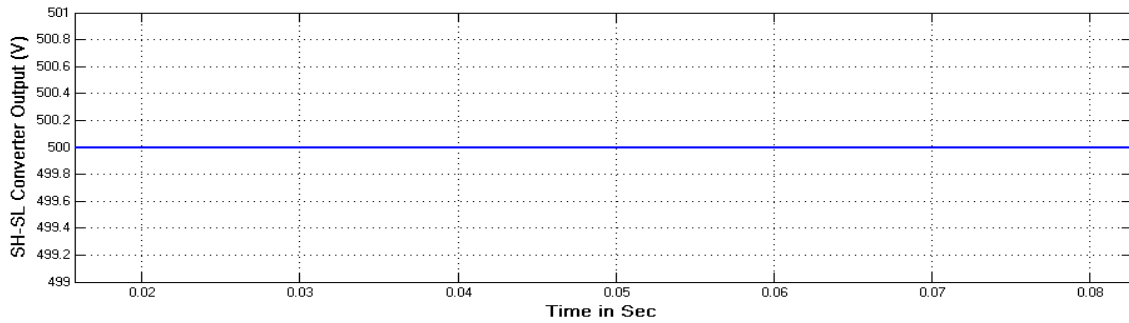


Fig. 14. Output voltage of Hybrid converter

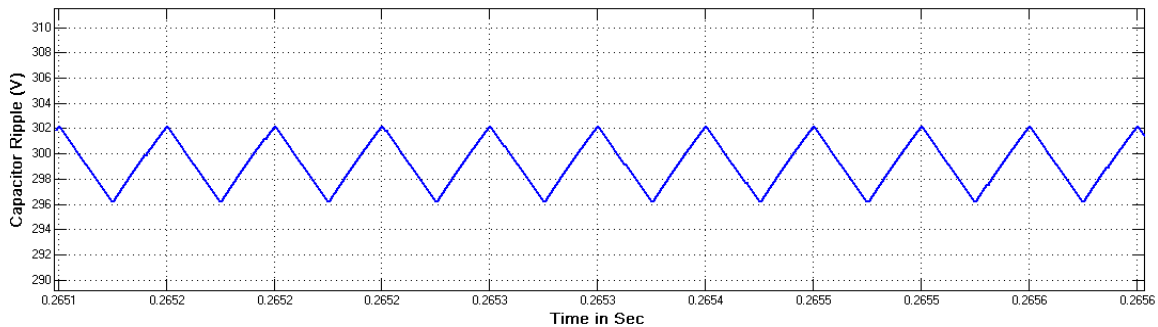


Fig. 15. Change in inductor current

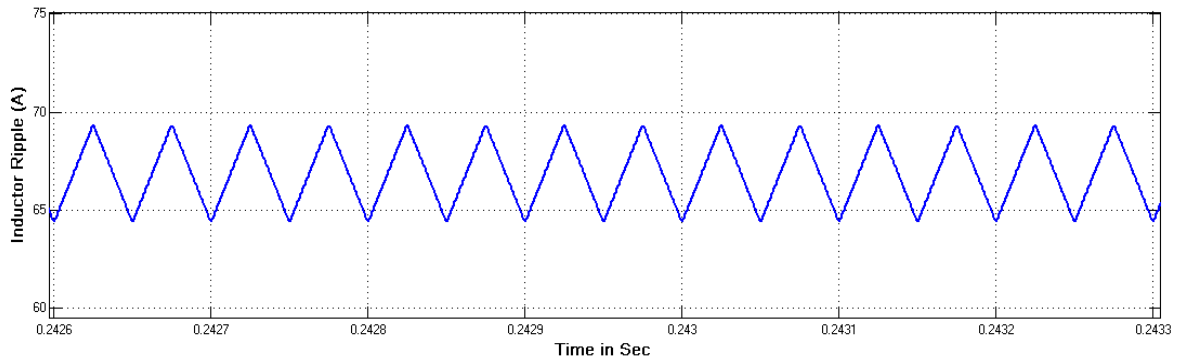


Fig. 16. Change in Capacitor voltage

III. RESULT ANALYSIS

A. PV with SH-SLC and SRM with fixed torque and speed

The voltage wave shape at the output of solar system is shown in figure 13. The PV system yields a voltage of 100V. This output of PV system will be the source to SH-SL converter. SH-SL converter is designed to give five times the output voltage. The output of PV system is increased by five times to 500V as in figure 14. Inductor ripple current and the capacitor ripple voltage are shown in figure 15 and figure 16 respectively.

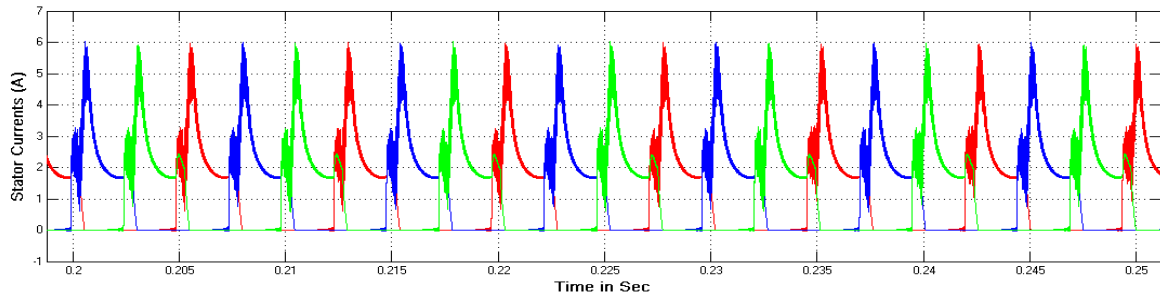


Fig. 17. SRM stator excitation currents

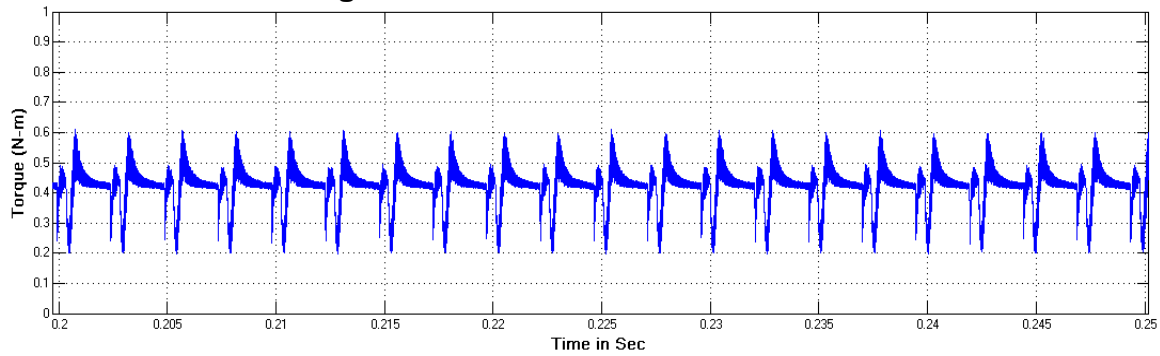


Fig. 18. SRM torque characteristics

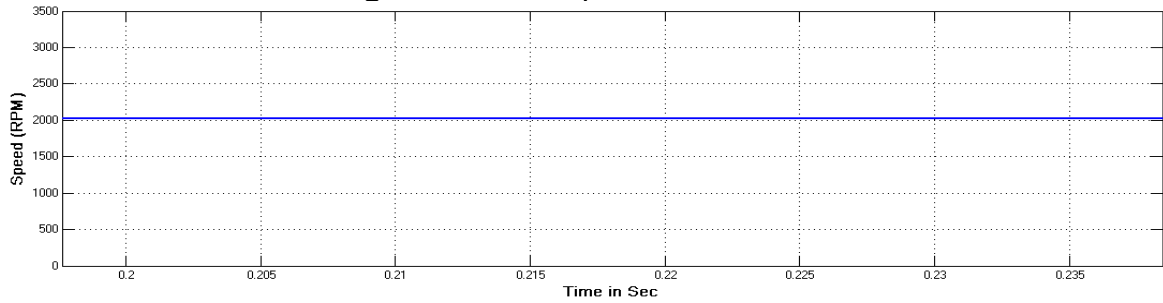


Fig. 19. SRM rotor running speed

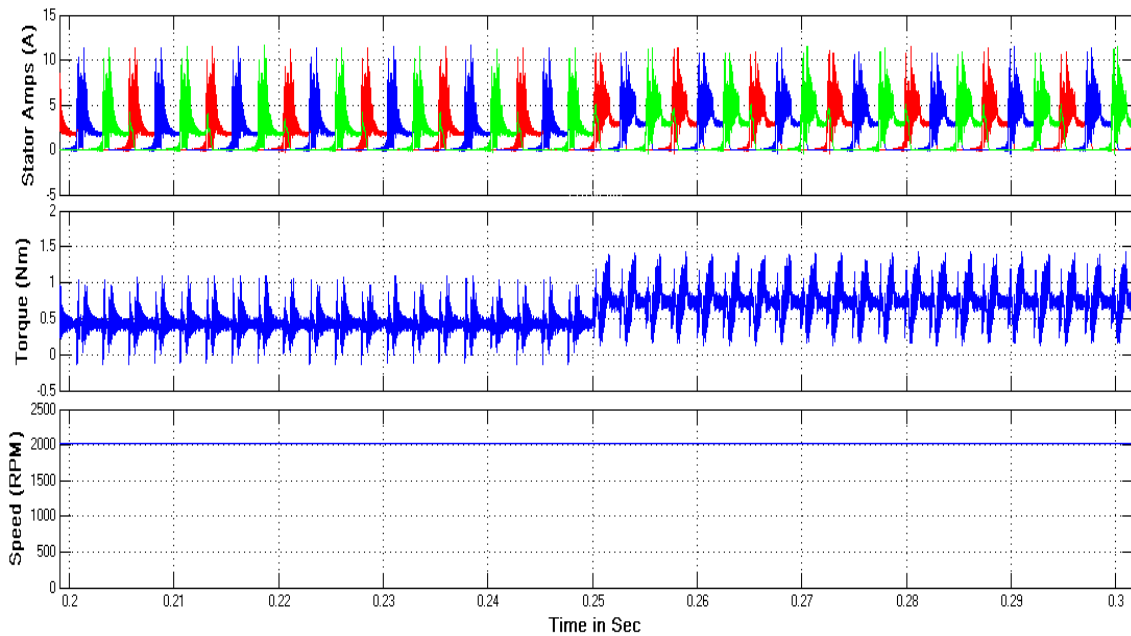


Fig. 20. Stator currents, Torque and speed of SRM drive

Switched Reluctance Motor characteristics to drive an electric vehicle are shown in figures 17, 18 and 19. The stator currents, torque and speed curves are shown respectively. The rotor speed is constant at 2000rpm when the stator is excited with 6A current.

B. PV with SH-SLC and SRM with varied torque and fixed speed

PV and SH-SL converter output remains same as shown in case-1. Switched Reluctance Motor characteristics to drive an electric vehicle are shown in figure 20. The stator currents, torque and speed curves are shown respectively. The rotor speed is constant at 2000rpm when the stator is excited. The rotor speed is constant at 2000rpm when the stator is excited and with variable torque condition. Though the torque is changed at 0.25 sec, the speed does not vary.

IV. CONCLUSION

During last few years, there is a constant effort from the field of power electronics to meet the challenges while using renewable energy sources. Electric vehicles are latest trends to replace traditional IC engine transport which pollutes the environment. This article demonstrates the solar-PV with symmetrical hybrid – switched inductor boost converter and traction switched reluctance motor. The gain of SH-SL DC-DC converter is better compared to other converter topologies. The SH-SL DC-DC converter is analyzed, compared with existing topologies and details are presented. SH-SL DC-DC is run in closed-loop operating mode, and closed-loop speed control is adopted for SRM drive. Design of SH-SL DC-DC is discussed in the article. Switched reluctance traction motor stator coils are excited from asymmetrical converter. SRM drive running with fixed speed applied with fixed torque and variable torque is analyzed for drive train application.

CONFLICT OF INTEREST

"The authors declare no conflict of interest".

AUTHOR CONTRIBUTIONS

Ravi Kiran Dasari conducted the research; analyzed the data; wrote the paper. Dr. Godwin Immanuel supervised the work; all authors had approved the final version.

REFERENCES

- [1] A. Campoccia, L. Dusonchet, E. Telaretti, and G. Zizzo, "Comparative analysis of different supporting measures for the production of electrical energy by solar PV and Wind systems: four representative European cases," *Solar Energy*, vol. 83, no. 3, pp. 287–297, 2009.
- [2] M. Liserre, T. Sauter, and J. Y. Hung, "Future energy systems: integrating renewable energy sources into the smart power grid through industrial electronics," *IEEE Industrial Electronics Magazine*, vol. 4, no. 1, pp. 18–37, 2010.
- [3] H. M. Hsu and C. T. Chien, "Multiple Turn Ratios of On-Chip Transformer With Four Intertwining Coils," *IEEE Trans. Electron Devices*, vol. 61, no. 1, pp. 44–47, Jan. 2014.
- [4] X. Zhang, C. C. Yao, C. Li, L. X. Fu, F. Guo, and J. Wang, "A Wide Bandgap Device-Based Isolated Quasi-Switched-Capacitor DC/DC Converter," *IEEE Trans. Power Electron.*, vol. 29, no. 5, pp. 2500–2510, May. 2014.
- [5] B. Gu, J. Dominic, J. S. Lai, Z. Zhao, and C. Liu, "High Boost Ratio Hybrid Transformer DC–DC Converter for Photovoltaic Module Applications," *IEEE Trans. Power Electron.*, vol. 28, no. 4, pp. 2048–2058, Apr. 2013.
- [6] H. S. Kim, J. W. Baek, M. H. Ryu, J. H. Kim, and J. H. Jung, "The High-Efficiency Isolated AC–DC Converter Using the Three-Phase Interleaved LLC Resonant Converter Employing the Y-Connected Rectifier," *IEEE Trans. Power Electron.*, vol. 29, no. 8, pp. 4017–4028, Aug. 2014.

- [7] L. Schmitz, D. C. Martins and R. F. Coelho, "Comprehensive Conception of High Step-Up DC–DC Converters With Coupled Inductor and Voltage Multipliers Techniques," in *IEEE Transactions on Circuits and Systems I: Regular Papers*, vol. 67, no. 6, pp. 2140-2151, June 2020, doi: 10.1109/TCSI.2020.2973154.
- [8] P. H. Tseng, J. F. Chen, and Y. P. Hsieh, —A novel active clamp high step-up DC-DC converter with coupled-inductor for fuel cell system,|| in *Proc. IEEE IFEEC*, 2013, pp. 326-331.
- [9] Y. Zhao, W. H. Li, and X. N. He, —Single-Phase Improved Active Clamp Coupled-Inductor-Based Converter With Extended Voltage Doubler Cell,|| *IEEE Trans. Power Electron.*, vol. 27, no. 6, pp. 2869-2878, Jun. 2012.
- [10] V. K. Goyal and A. Shukla, "Isolated DC–DC Boost Converter for Wide Input Voltage Range and Wide Load Range Applications," in *IEEE Transactions on Industrial Electronics*, vol. 68, no. 10, pp. 9527-9539, Oct. 2021, doi: 10.1109/TIE.2020.3029479
- [11] M. N. Gitau, G. P. Adam, L. Masike and M. W. K. Mbukani, "Unified Approach for Synthesis and Analysis of Non-Isolated DC-DC Converters," in *IEEE Access*, vol. 9, pp. 120088-120109, 2021, doi: 10.1109/ACCESS.2021.3108191.
- [12] G. H. de Alcântara Bastos, L. F. Costa, F. L. Tofoli, G. V. Torrico Bascopé and R. P. Torrico Bascopé, "Nonisolated DC–DC Converters With Wide Conversion Range for High-Power Applications," in *IEEE Journal of Emerging and Selected Topics in Power Electronics*, vol. 8, no. 1, pp. 749-760, March 2020, doi: 10.1109/JESTPE.2019.2892977.
- [13] T. Meng, S. Yu, H. Q. Ben, and G. Wei, —A Family of Multilevel Passive Clamp Circuits With Coupled Inductor Suitable for Single-Phase Isolated Full-Bridge Boost PFC Converter,|| *IEEE Trans. Power Electron.*, vol. 29, no. 8, pp. 4348-4356, Aug. 2014.
- [14] Y. P. Hsieh, J. F. Chen, T. J. Liang, L. S. Yang, —Novel High Step-Up DC–DC Converter With Coupled-Inductor and Switched-Capacitor Techniques||, *IEEE Trans. Ind. Electron.*, vol. 59, no. 2, pp. 998–1007, Feb. 2012.
- [15] J. H. Lee, T. J. Liang, J. F. Chen, —Isolated Coupled-Inductor-Integrated DC–DC Converter With Nondissipative Snubber for Solar Energy Applications,|| *IEEE Trans. Ind. Electron.*, vol. 61, no. 7, pp. 3337-3348, Jul. 2014.
- [16] J. Lei, Z. Xi, C. L. Yin, M. Chris, S. Q. Li, and M. Y. Zhang, —A novel soft-switching bidirectional DC-DC converter with coupled inductors,|| in *Proc. IEEE APEC*, 2013 pp. 3040-3044.
- [17] B. L. Narasimharaju, S. P. Dubey, and S. P. Singh, —Coupled inductor bidirectional DC-DC converter for improved performance,|| in *Proc. IEEE IECD*, 2010, pp. 28-33.
- [18] F. Yang, X. B. Ruan, Q. Ji, and Z. H. Ye, —Input DM EMI filter design of interleaved CRM Boost PFC converter with coupled inductor,|| in *Proc. IEEE ECCE*, 2011, pp. 2614-2621.
- [19] K. Umetani, S. Arimura, T. Hirano, J. Imaoka, and M. Yamamoto, —Evaluation of the Lagrangian method for deriving equivalent circuits of integrated magnetic components: A case study using the integrated winding coupled inductor,|| in *Proc. IEEE ECCE*, 2013, pp. 495-502.
- [20] F. Yang, X. B. Ruan, Y. Yang, and Z. H. Ye, —Interleaved Critical Current Mode Boost PFC Converter With Coupled Inductor,|| *IEEE Trans. Power Electron.*, vol. 26, no. 9, pp. 2404-2413, Sep. 2011.
- [21] B. R. Lin and J. J. Chen, —Analysis and implementation of a soft switching converter with high-voltage conversion ratio,|| *Proc. IET-Power Electron.*, vol. 1, no. 3, pp. 386–394, Sep. 2008.
- [22] L. S. Yang, T. J. Liang, and J. F. Chen. —Transformerless DC–DC Converters With High Step-Up Voltage Gain ,|| *IEEE Trans. Ind. Electron.*, vol. 56, no. 8, pp. 3144–3152, Aug. 2009.
- [23] G. Li, J. Xia, K. Wang, Y. Deng, X. He and Y. Wang, "Hybrid Modulation of Parallel-Series \$LLC\$ Resonant Converter and Phase Shift Full-Bridge Converter for a Dual-Output DC–DC Converter," in *IEEE Journal of Emerging and Selected Topics in Power Electronics*, vol. 7, no. 2, pp. 833-842, June 2019, doi: 10.1109/JESTPE.2019.2900700.
- [24] Y. Liang, H. Zhang, M. Du and K. Sun, "Parallel coordination control of multi-port DC-DC converter for stand-alone photovoltaic-energy storage systems," in *CPSS Transactions on Power Electronics and Applications*, vol. 5, no. 3, pp. 235-241, Sept. 2020, doi: 10.24295/CPSSTPEA.2020.00020.
- [25] K. Tesaki and M. Hagiwara, "Control and Experimental Verification of a Bidirectional Nonisolated DC–DC Converter Based on Switched-Capacitor Converters," in *IEEE Transactions on Power Electronics*, vol. 36, no. 6, pp. 6501-6512, June 2021, doi: 10.1109/TPEL.2020.3040070D.
- [26] Bao, A. Kumar, X. Pan, X. Xiong, A. R. Beig and S. K. Singh, "Switched Inductor Double Switch High Gain DC-DC Converter for Renewable Applications," in *IEEE Access*, vol. 9, pp. 14259-14270, 2021, doi: 10.1109/ACCESS.2021.3051472.

- [27] B. Axelrod, Berkovich, —Switched-capacitor/ switched-inductor structures for getting transformerless hybrid DC–DC PWM converters, *IEEE Trans. Circuits Syst. I, Reg. Papers*, vol. 55, no. 2, pp. 687–696, Mar. 2008.
- [28] L. Yang, T. Liang and J. Chen, "Transformerless DC–DC Converters With High Step-Up Voltage Gain," in *IEEE Transactions on Industrial Electronics*, vol. 56, no. 8, pp. 3144-3152, Aug. 2009
- [29] Y. Tang, D. Fu, T. Wang and Z. Xu, "Hybrid Switched-Inductor Converters for High Step-Up Conversion," in *IEEE Transactions on Industrial Electronics*, vol. 62, no. 3, pp. 1480-1490, March 2015.
- [30] V. Telukunta, J. Pradhan, A. Agrawal, M. Singh and S. G. Srivani, "Protection challenges under bulk penetration of renewable energy resources in power systems: A review," in *CSEE Journal of Power and Energy Systems*, vol. 3, no. 4, pp. 365-379, Dec. 2017
- [31] V. Lojpur and I. L. J. Validžić, "Influence of Different Light Sources, Light Intensities, and Water Flow Lens (WFL) System on Dye-Sensitized Solar Cell Performances," in *IEEE Journal of Photovoltaics*, vol. 9, no. 2, pp. 492-498, March 2019
- [32] V. Karthikeyan, S. Kumaravel and G. Gurukumar, "High Step-Up Gain DC–DC Converter With Switched Capacitor and Regenerative Boost Configuration for Solar PV Applications," in *IEEE Transactions on Circuits and Systems II: Express Briefs*, vol. 66, no. 12, pp. 2022-2026, Dec. 2019
- [33] C. Jin, X. Sheng and P. Ghosh, "Optimized Electric Vehicle Charging With Intermittent Renewable Energy Sources," in *IEEE Journal of Selected Topics in Signal Processing*, vol. 8, no. 6, pp. 1063-1072, Dec. 2014
- [34] K. Rajashekara, "Present Status and Future Trends in Electric Vehicle Propulsion Technologies," in *IEEE Journal of Emerging and Selected Topics in Power Electronics*, vol. 1, no. 1, pp. 3-10, March 2013
- [35] J. Zhu, K. W. E. Cheng, X. Xue and Y. Zou, "Design of a New Enhanced Torque In-Wheel Switched Reluctance Motor With Divided Teeth for Electric Vehicles," in *IEEE Transactions on Magnetics*, vol. 53, no. 11, pp. 1-4, Nov. 2017
- [36] J. Fan *et al.*, "Thermal Analysis of Permanent Magnet Motor for the Electric Vehicle Application Considering Driving Duty Cycle," in *IEEE Transactions on Magnetics*, vol. 46, no. 6, pp. 2493-2496, June 2010.